Resting-state EEG classification for PNES diagnosis

Chiara Zucco[1][0000−0003−0048−0457], Barbara Calabrese[1][0000−0003−2123−8221], Rossana Mancuso[1], Miriam Sturniolo[2], Antonio Gambardella[2][0000−0001−7384−3074], Mario Cannataro[1][0000−0003−1502−2387]

[1] Data Analytics Research Center, Department of Medical and Surgical Sciences, University "Magna Græcia" of Catanzaro, Italy
[2] Clinic of Neurology, Policlinico Mater Domini, University "Magna Græcia" of Catanzaro, Italy
chiara.zucco@unicz.it, calabreseb@unicz.it, cannataro@unicz.it

Abstract. Psychogenic Non-Epileptic Seizure (PNES) represents a neurological disorder often diagnosed and pharmacologically treated as epilepsy. PNES subjects show the same symptoms as epileptic patients but do not have an EEG characterized by ictal patterns during psychogenic seizures. Diagnosis requires an EEG video, but this methodology is very time-consuming and dispensable in both time and cost. Our paper aims to define a novel methodology to support the clinical diagnosis of PNES by analyzing electroencephalographic (EEG) signals obtained in resting conditions. In this case, it is unnecessary to induce seizures in the subjects. A software pipeline was implemented based on robust feature extraction methods used in quantitative EEG analysis in the clinical setting, integrating them with machine learning classifiers. Unlike other similar works, the methodology was tested on a large dataset consisting of 225 EEGs (75 healthy, 75 PNES and 75 subjects with epilepsy), showing that it has a classification accuracy greater than 85%.

Keywords: Epilepsy · PNES · EEG · Data Mining · Classification

1 Introduction

There is a growing body of literature on the COVID-19 pandemic's impact on patients with chronic neurological conditions. These studies include the direct effect of infection with the novel SARS-CoV-2 virus and the wide-reaching societal implications of the pandemic. This global crisis has had a profound psychological impact, perhaps more severe in people with seizures. Patients with more frequent attacks at baseline were more susceptible to worsening and increased stress, and barriers to care appeared to play significant roles in their deterioration. In [13], the authors reported an aggravation of the seizure frequency in PNES (Psychogenic Non-Epileptic Seizures) patients, a vulnerable group of people during this pandemic COVID-19. Among a cohort of 18 subjects with PNES, 22.2% reported an improvement in seizure control during the peak of the COVID-19 pandemic in New York City [11].

ICCS Camera Ready Version 2022
To cite this paper please use the final published version:
DOI: 10.1007/978-3-031-08754-7_58

Psychogenic non-epileptic seizures are sudden behavioural changes simulating epileptic seizures but without EEG ictal patterns, caused by psychic alterations [3], [7], [1], [12].

The gold standard for PNES diagnosis is video-electroencephalography (video-EEG), during which seizures are recorded spontaneously or provoked by stimulation techniques.

EEG recordings alone are insufficient to diagnose PNES because an ictal scalp EEG may reveal no epileptic characteristics during simple partial seizures or mesial frontal lobe seizures. In addition, the discrimination between non-epileptic seizures and healthy subjects can be challenging. Moreover, differential diagnosis cannot rely only on clinical features of PNES because most of the signs are associated with epileptic seizures. PNES patients simulate the different types of epileptic seizures but no epileptic seizures EEG patterns.

A wrong diagnosis with epilepsy may direct to treatments through anti-epileptic drugs. However, it has been assessed that the correct diagnosis of PNES is usually postponed for an average of seven years [5], with a profound consequence on patients' and caregivers' quality of life [10].

Additionally, EEG video-monitoring is highly time-consuming and labour intensive and, therefore, relatively expensive and limited in availability; thus, alternative diagnostic procedures are necessary to support neurologist diagnosis and proper pharmacological treatment.

Despite many efforts made, no bio-marker of PNES has yet been identified. However, in [15], the authors sustain patients with PNES have a stable frequency of rhythmic movements, about (5Hz).

Continuous wavelet transform is used in [6] to process controls (CNT) and PNES EEG signals. In [14], a novel machine learning (ML) pipeline for classifying EEG epochs of PNES and healthy controls is described. The authors propose a semi-automatic signal processing technique and a supervised ML classifier to support the discriminative clinical diagnosis of PNES. In addition, they extracted statistical features like the mean, standard deviation, kurtosis, and skewness from a power spectral density (PSD) map split up into the five EEG bands. Finally, they compared three different supervised ML algorithms, namely, the Support Vector Machine (SVM), Linear Discriminant Analysis (LDA), and Bayesian network (BN), to classify control vs PNES subjects. The authors tested the proposed methodology on a small dataset of 20 EEG signals (10 PNES and 10 control), reaching an average accuracy above 90%.

To the best of our knowledge, only a few studies have investigated semi-automatic or automatic machine learning-based approaches for discrimination between healthy, epileptic and PNES subjects by only considering EEG recordings. Furthermore, the current study is one of the few in which an EEG dataset without any correlated video-EEG PNES marker has been analyzed to discriminate PNES via EEG.

Specifically, this paper proposes a novel and semi-automatic pipeline to discriminate between healthy, PNES and epileptics subjects based on the extraction of spectral features from EEG signals and classification through Machine

ICCS Camera Ready Version 2022
To cite this paper please use the final published version:
DOI: 10.1007/978-3-031-08754-7_58

Learning-based approaches. To design a software pipeline that allows discrimination, we have implemented different classifiers, i.e. Light Gradient Boosting Machine, Random forest, Decision tree and Linear Discriminant Analysis. We analyzed 75 EEGs for each class (healthy, PNES and epileptic) in our work. The results achieved in terms of classification accuracy are higher than 80%.

The paper is organized as follows: Section 2 introduces the implemented EEG methodologies; Section 3 presents and discusses the results obtained from the proposed software pipeline. Finally, Section 4 concludes the paper.

2 Methods

In this section we describe the methodologies implemented for EEG analysis. Figure 1 illustrates the main steps that are:

- **EEG acquistion**: This module performs standard EEG acquisition according to the 10/20 international standard;
- **Pre-processing**: This module performs digital filtering and EEG segmentation into epochs;
- **Features extraction**: The Power Spectral Density (PSD) function is estimated for each channel using the classical Welch method. From PSD functions, cumulative power coefficients in clinical EEG bands are calculated to create a features vector to feed in input to the classifier module;
- **EEG classification**: the framework implements a pool of classifiers, such as Linear Discriminant Analysis, Decision Tree, Random Forest and Light Gradient Boosting Machine to discriminate healthy, PNES and epileptic EEGs acquired in resting conditions.

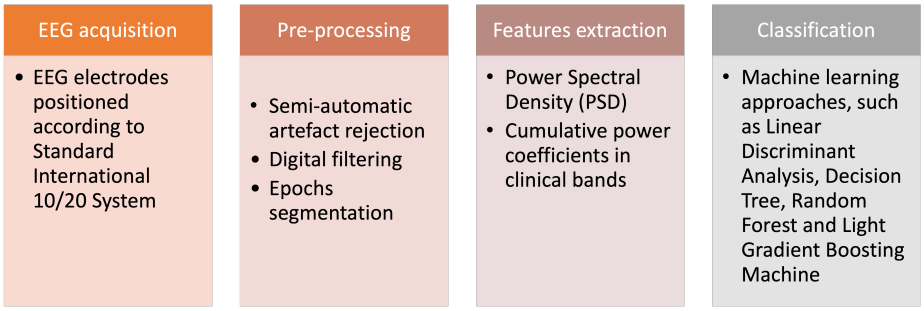

Fig. 1. EEG data analysis pipeline.

2.1 EEG Pre-processing

In general, EEG signals acquisition is very difficult because the signals are very weak and are contaminated by environmental noise or distorted by physiological

ICCS Camera Ready Version 2022
To cite this paper please use the final published version:
DOI: 10.1007/978-3-031-08754-7_58

artefacts (i.e. ocular and muscle artefacts). Therefore, removing noise is a fundamental step in EEG signals processing and classification. A proper data cleaning may improve the signal to noise ratio and allow for the discrimination of the most meaningful features from the EEG signals. In clinical practice, the artefacts' detection is performed visually by trained neurologists by discarding contaminated EEG epochs. Therefore, the pre-processing stage is operator-dependent, monotonous and time-consuming.

In this study, each EEG recording was inspected by a qualified neurologist to mark noise and artefact corrupted epoch (see Figure 2). Afterwards, all EEG data were pre-processed using digital filtering techniques. Specifically, we have employed a Butterworth band-pass filter (0.1-70 Hz) and a notch filter (cut-off frequency 50 Hz) to reduce high-frequency artefacts and power-line interference (see Figure 3).

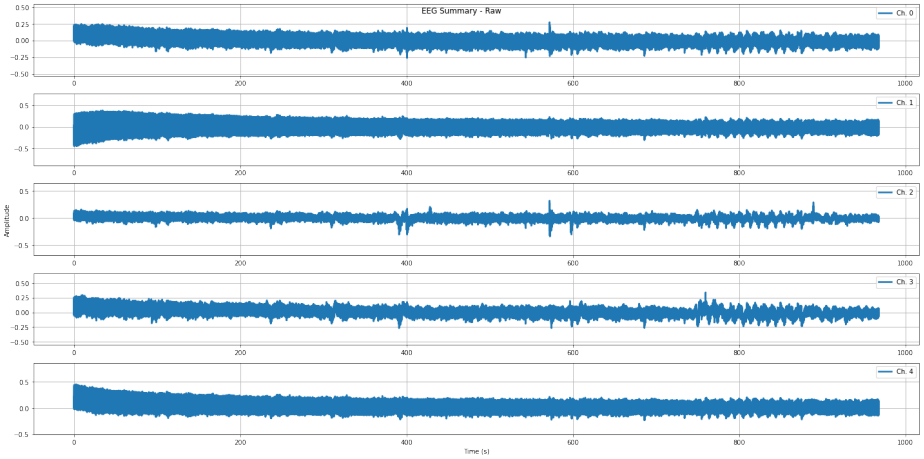

Fig. 2. An example of EEG signals acquired from some electrodes positioned on the frontal and central lobes (the time of acquisition is indicated on the x-axis; the amplitude values in mV are reported on the y-axis).

After noise removal, EEG signals were segmented in EEG epochs of 10 seconds in order to apply the subsequent features extraction methods on each epoch. Moreover, the segmentation of the signal in epochs is helpful as it allows a more accurate analysis of the variations of the EEG signal at the local level. However, the EEG signal is strongly stationary. Therefore, to apply the subsequent spectral analysis, it is necessary to segment it into epochs rather than analyze it for its entire duration. This operation also extends the dataset without resorting to artificial methods, improving the classification process.

ICCS Camera Ready Version 2022
To cite this paper please use the final published version:
DOI: 10.1007/978-3-031-08754-7_58

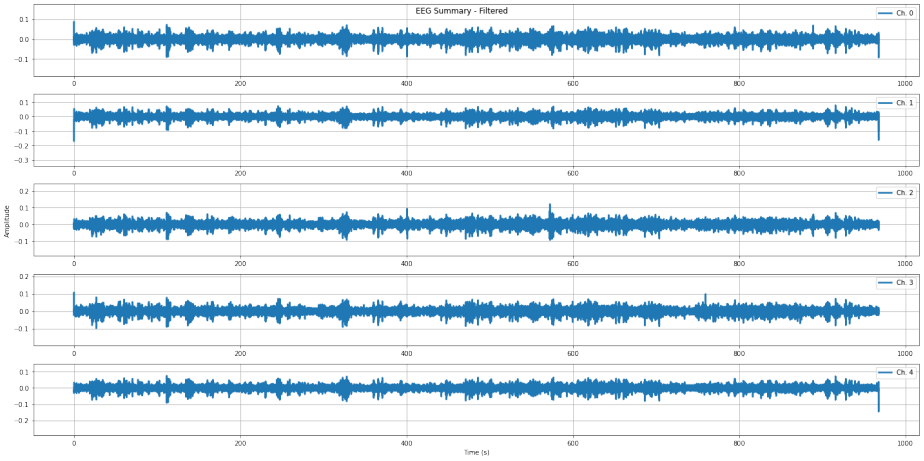

Fig. 3. An example of filtered EEG signals acquired from some electrodes positioned on the frontal and central lobes (the time of acquisition is indicated on the x-axis; the amplitude values in mV are reported on the y-axis).

2.2 EEG Features Extraction

After the pre-processing step, the next stage in the EEG software pipeline is the features extraction stage. As stated before, features extraction seeks to extract relevant information retained in the signals.

We decided to implement the Power Spectral Density (PSD) analysis because it is a robust extractor largely used for EEG quantitative analysis. Specifically, among the several methods for PSD estimation reported in the literature, we have chosen Welch's method. It is a well-known non-parametric method for PSD computation. Let $x[n],\ n = 0, , N-1$ be the samples from an EEG epoch. The evaluation of PSD by using Welch's method consists of the following steps:

- the original EEG epoch is divided into N sections (possibly overlapped O) of equal lengths M;

$$x\lfloor n \rfloor = x\lfloor n + iO \rfloor \qquad i = 0, \dots K-1, \text{ and } n = 0, \dots N-1 \tag{1}$$

- a window is applied to each section, and then the periodogram on the windowed sections is calculated. The periodogram is defined as:

$$\tilde{S}_{xx}(k) = \frac{1}{N} \left| \sum_{n=0}^{N-1} x(n) e^{-\frac{2jkn}{N}} \right|^2 . \tag{2}$$

- the periodograms are averaged from the K sections in order to obtain an estimator of the spectral density

$$P_{yx}(f) = \frac{1}{K} \sum_{i=0}^{K-1} P_i(f) \tag{3}$$

ICCS Camera Ready Version 2022
To cite this paper please use the final published version:
DOI: 10.1007/978-3-031-08754-7_58

Where P_{yx} estimates the cross power spectral density of two discrete-time signals, x and y, the Welch method eliminates the tradeoff between spectral resolution and variance by allowing the segments to overlap. If a high-frequency resolution is needed, the record could split into a small number N of segments of length L. Our analysis uses a segment with a 50% overlap for the first step and the Hamming window in the second step.

In this paper, we extracted power spectral density (PSD) of classical frequency bands from around 1 Hz to 70 Hz. Specifically, delta (1-4 Hz), theta (4-8 Hz), alpha (8-13 Hz), beta (13-30 Hz), gamma (30-70 Hz) bands have been considered.

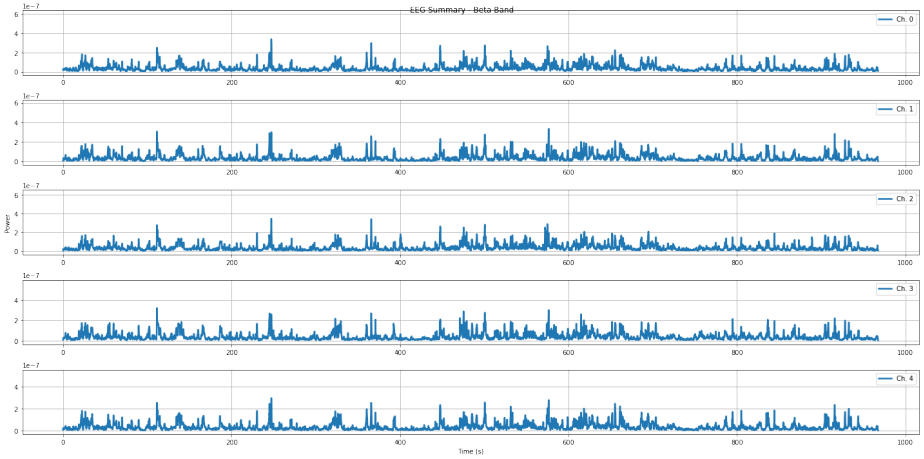

Fig. 4. EEG signals power in the beta band evaluated for all epochs.

The main processing steps of our feature extraction approach can be summarized as:

- Power Spectral Density (PSD) was estimated through Welch method;
- from PSD matrix output, we evaluated cumulative power for all EEG frequencies;
- from PSD matrix output, we selected five frequency sub-bands;
- for each band (delta, teta, alpha, beta, gamma) we computed cumulative power.

Figure 4 shows an example of cumulative power in beta band for all epochs extracted from an EEG signal.

All features extracted (six power cumulative coefficients for all epochs for all EEGs) are arranged into the features vector.

ICCS Camera Ready Version 2022
To cite this paper please use the final published version:
DOI: 10.1007/978-3-031-08754-7_58

2.3 EEG classification

Several supervised Machine Learning algorithms and ensemble techniques have been tested to discriminate CNT (control) EEG (healthy) from PNES EEG and epileptic EEG: LDA, Decision Trees, Random Forest and Gradient Boosting.

LDA classifier finds an optimal linear transformation that maximizes the class separability. LDA generates a linear combination of data sets that permits the largest mean differences between the desired classes. It works well when the feature vector is multivariate normally distributed in each class group, and different groups have a common covariance.

In decision trees algorithm [9] knowledge is gained through a set of rules, structured in a tree form. Random forest [4] is a bagging ensemble of decision trees while in Light Gradient Boosted Machine (LGBM) [8] a boosting ensemble of decision trees is built by minimizing a differentiable loss function through gradient descent optimization algorithm. Evaluation was performed through a 70%/30% Random Train Test Split.

3 Results

In this study, we analyzed EEG recordings from 75 patients with PNES, 75 healthy patients referred to as CNT (controls) and 75 epileptic patients. EEG acquisitions were performed from the Operative Unit of Neurology, Mater Domini Polyclinic, University of Catanzaro, Italy. PNES patients were diagnosed according to a video-EEG registration of a typical episode, with EEG showing neither concomitant ictal activity nor post-ictal. None of the subjects was on chronic medication or had received any drug up to 24 hours. The study was conducted following the Declaration of Helsinki and formally approved by the local Medical Research Ethics Committee. Participants were comfortably seated in a semi-darkened room and with open eyes. EEG recordings were acquired using 19 Ag/AgCl surface electrodes positioned according to the International 10/20 System (see Figure 5). Recordings were performed with an Xltek Brain Monitor EEG Amplifier with a sampling rate of 256 Hz, a high-pass filter at 0.5 Hz, a low-pass filter at 70 Hz, and a 50 Hz notch filter.

All the electrode-skin impedance has been kept below 5 KΩ. The EEG data were recorded in a resting condition. The average EEG acquisition duration is between 10 and 20 minutes. The signals have been segmented in epochs lasting 10 seconds. So an average number of 105 epochs has been obtained for each channel for each subject.

Then for each EEG epoch, the six cumulative power coefficients (introduced in section 2) were evaluated. The features vector has the following dimension: the number of cumulative power coefficients (6) times the number of epochs (an average of 105 epochs for each EEG) times the number of channels (19) times the number of subjects (225).

The training and testing of the different machine learning models described in section 2 was conducted through the python PyCaret library (available online at https://pycaret.org.)

ICCS Camera Ready Version 2022
To cite this paper please use the final published version:
DOI: 10.1007/978-3-031-08754-7_58

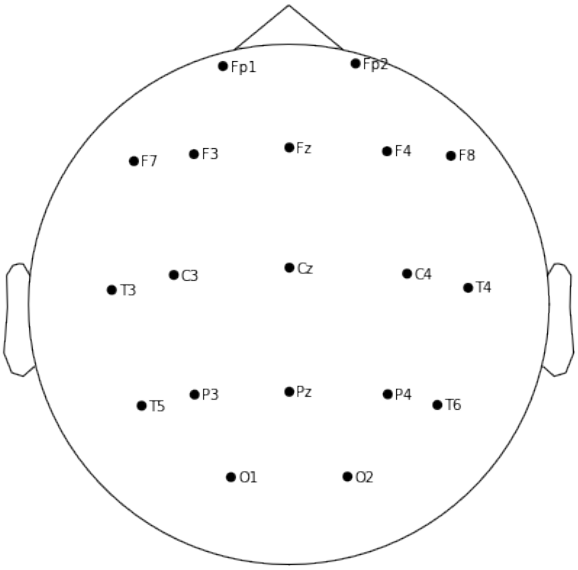

Fig. 5. EEG electrodes montage according to the 10/20 International Standard.

For the evaluation of the multiclass predictive models, several comparative metrics were chosen, including accuracy and AUC (The Area Under the Curve) with a One vs Rest (OvR) strategy [2].

Accuracy represents the proportion of instances correctly predicted by the algorithm. For example, in the case of multiclass classification with OvR strategy, we indicated with $TCNT$, $TEPI$ and $TPNES$, the number of CNT, EPI and PNES subjects that the model correctly predicts, and $FCNT$, $FEPI$ and $FPNES$, the number of CNT, EPI and PNES subjects misclassified by the model. Therefore, we can define the accuracy as:

$$Accuracy = \frac{TCNT + TEPI + TPNES}{TCNT + TEPI + TPNES + FCNT + FEPI + FPNES}$$

AUC is one of the evaluation criteria of the ability of a classifier to distinguish between classes. It is used as a summary of the Receiver Operating Characteristic (ROC) curve. The ROC curve reveals the discrimination capability by plotting the True Positive Rate against the False Positive Rate in threshold values. The area under the ROC curve (AUC) provides an aggregate measure of ROC performance. In an OvR strategy, the ROC curve was considered separately for each class (see Figure 6, where we plotted ROC curves for the LGBM classifier and each class). Micro and macro-average ROC curves were also considered as global measures.

ICCS Camera Ready Version 2022
To cite this paper please use the final published version:
DOI: 10.1007/978-3-031-08754-7_58

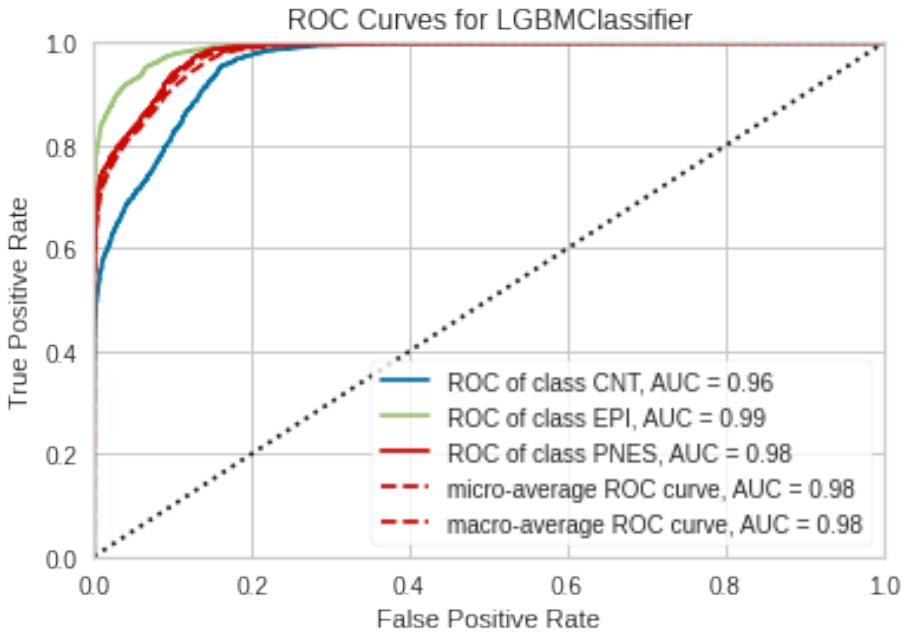

Fig. 6. ROC Curves for LGBM Classifier.

In Table 1 Accuracy and micro-average Area Under the Curve (AUC) of the classifier models are compared. Best values are highlighted in bold. The results show that LGBM reached the best performance.

Table 1. Accuracy and AUC of the considered models.

Model	Accuracy	AUC
Light Gradient Boosting Machine	**0.86**	**0.98**
Random Forest	0.85	0.95
Decision Tree	0.74	0.81
Linear Discriminant Analysis	0.45	0.65

The good performances of the LGBM model are also confirmed by the precision and recall curve, reported in Figure 7. It shows a good tradeoff between false positive and false negative rates.

Further insights regarding the most discriminative features and the separability of each of the classes are shown for the most performing model, i.e. LGBM. In particular, by combining the results reported in the confusion matrix w.r.t. the test set (Table 2), the OvR ROC curves and the micro and macro average ROC curves in Figure 6, and the percentage of errors committed by class, as

ICCS Camera Ready Version 2022
To cite this paper please use the final published version:
DOI: 10.1007/978-3-031-08754-7_58

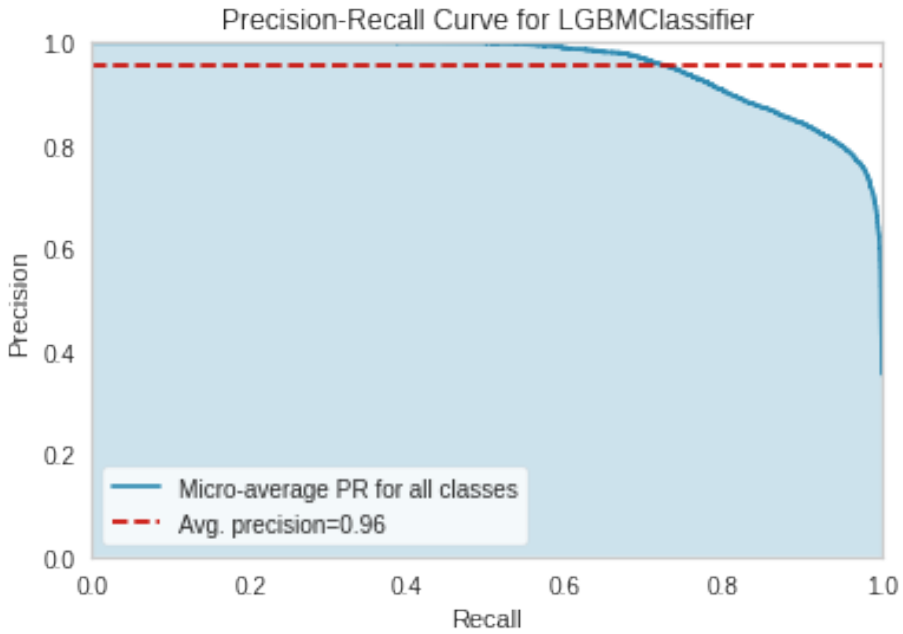

Fig. 7. Precision-Recall curve.

shown in Figure 8, it is possible to conclude that the EPI class was the one best discriminated by the model, with a 99% AUC and an error rate of 3%. In comparison, 10% of PNES subjects were erroneously classified as CNT, and 13% of CNT subjects were erroneously classified as PNES by the LGBM model.1

According to the results shown in Figure 9, the most significant features of the LGBM classifier are the cumulative power in the theta band in the Pz electrode and the gamma band.

4 Conclusions

In the neurological field, the diagnosis of PNES seizures requires considerable effort and time, as PNES patients show the same symptoms as people with epilepsy. Generally, PNES patients are diagnosed as epileptic and pharmacologically treated for several years before the correct diagnosis is made, with significant consequences for the patient. Therefore, we are trying to define new methodologies to support clinical diagnosis to reach an accurate diagnosis of PNES quickly. This work proposes a method for analyzing the EEG acquired in resting conditions with combined signal processing and machine learning techniques. Our analysis pipeline was tested on a massive dataset of approximately 225 subjects and produced classification accuracy results between control subjects, PNES and epileptics greater than 85%.

ICCS Camera Ready Version 2022
To cite this paper please use the final published version:
DOI: 10.1007/978-3-031-08754-7_58

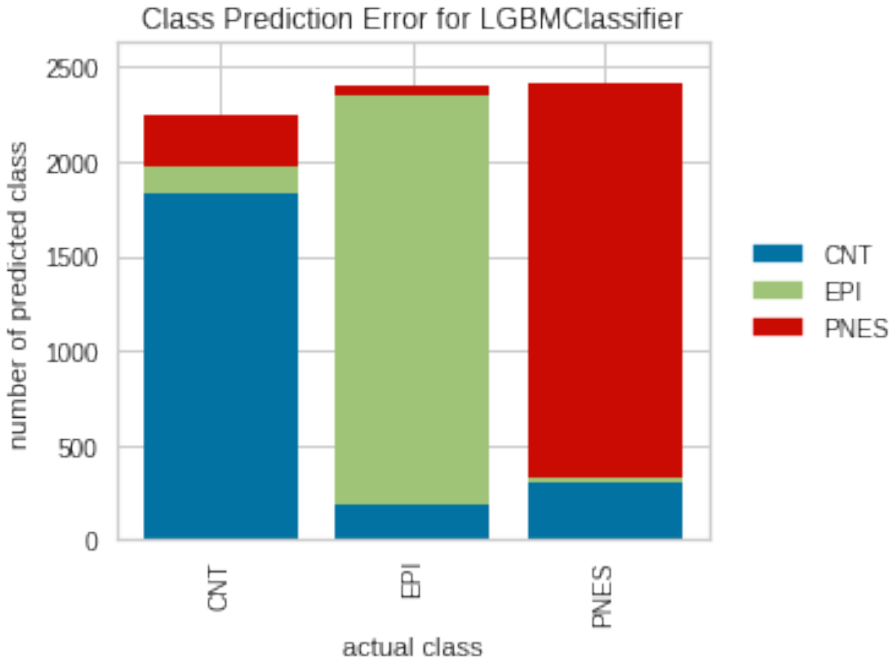

Fig. 8. Class predition errors for LGBM classifier.

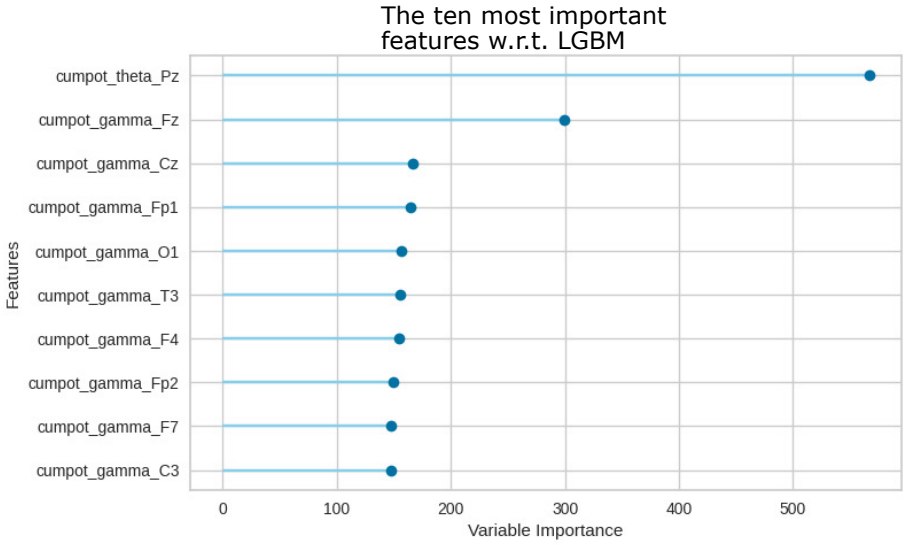

Fig. 9. The ten most important features w.r.t. LGBM.

ICCS Camera Ready Version 2022
To cite this paper please use the final published version:
DOI: 10.1007/978-3-031-08754-7_58

Table 2. LGBM Confusion Matrix.

		Predicted Class		
		CNT	**EPI**	**PNES**
Ground truth	**CNT**	1832	193	297
	EPI	149	2168	19
	PNES	256	35	2099

The results also show that the best model well discriminates EPI subjects among CNT and PNES, while 10% of PNES subjects were erroneously classified as CNT and 13% of CNT subjects as PNES.

The results show that the most significant features of the best performing model are the cumulative power in the theta band in the Pz electrode and the gamma band.

Further efforts will be made in future work to assess the impact of feature engineering on predictive performance by also considering Deep Learning algorithms.

References

1. Baslet, G., Roiko, A., Prensky, E.: Heterogeneity in psychogenic nonepileptic seizures: understanding the role of psychiatric and neurological factors. Epilepsy Behav. **17**(2), 236–241 (Feb 2010)
2. Bishop, C.M., Nasrabadi, N.M.: Pattern recognition and machine learning, vol. 4. Springer (2006)
3. Bodde, N.M.G., Brooks, J.L., Baker, G.A., Boon, P.A.J.M., Hendriksen, J.G.M., Mulder, O.G., Aldenkamp, A.P.: Psychogenic non-epileptic seizures–definition, etiology, treatment and prognostic issues: a critical review. Seizure **18**(8), 543–553 (Oct 2009)
4. Breiman, L.: Random forests. Machine learning **45**(1), 5–32 (2001)
5. Cianci, V., Ferlazzo, E., Condino, F., Mauvais, H.S., Farnarier, G., Labate, A., Latella, M.A., Gasparini, S., Branca, D., Pucci, F., Vazzana, F., Gambardella, A.,

ICCS Camera Ready Version 2022
To cite this paper please use the final published version:
DOI: 10.1007/978-3-031-08754-7_58

Aguglia, U.: Rating scale for psychogenic nonepileptic seizures: scale development and clinimetric testing. Epilepsy Behav. **21**(2), 128–131 (Jun 2011)
6. Gasparini, S., Beghi, E., Ferlazzo, E., Beghi, M., Belcastro, V., Biermann, K.P., Bottini, G., Capovilla, G., Cervellione, R.A., Cianci, V., Coppola, G., Cornaggia, C.M., De Fazio, P., De Masi, S., De Sarro, G., Elia, M., Erba, G., Fusco, L., Gambardella, A., Gentile, V., Giallonardo, A.T., Guerrini, R., Ingravallo, F., Iudice, A., Labate, A., Lucenteforte, E., Magaudda, A., Mumoli, L., Papagno, C., Pesce, G.B., Pucci, E., Ricci, P., Romeo, A., Quintas, R., Sueri, C., Vitaliti, G., Zoia, R., Aguglia, U.: Management of psychogenic non-epileptic seizures: a multidisciplinary approach. Eur. J. Neurol. **26**(2), 205–e15 (Feb 2019)
7. Gasparini, S., Campolo, M., Ieracitano, C., Mammone, N., Ferlazzo, E., Sueri, C., Tripodi, G.G., Aguglia, U., Morabito, F.C.: Information Theoretic-Based interpretation of a deep neural network approach in diagnosing psychogenic Non-Epileptic seizures. Entropy **20**(2), 43 (Jan 2018)
8. Ke, G., Meng, Q., Finley, T., Wang, T., Chen, W., Ma, W., Ye, Q., Liu, T.Y.: Lightgbm: A highly efficient gradient boosting decision tree. Advances in neural information processing systems **30** (2017)
9. Quinlan, J.R.: Induction of decision trees. Machine learning **1**(1), 81–106 (1986)
10. Reuber, M., Kral, T., Kurthen, M., Elger, C.E.: New-onset psychogenic seizures after intracranial neurosurgery. Acta Neurochir. **144**(9), 901–7; discussion 907 (Sep 2002)
11. Rosengard, J., Ferastraoaru, V., Donato, J., Haut, S.: Psychogenic nonepileptic seizures during the covid-19 pandemic in new york city - a distinct response from the epilepsy experience. Epilepsy Behav. **123**, 37–37 (2021). https://doi.org/10.1016/j.yebeh.2021.108255
12. Uliaszek, A.A., Prensky, E., Baslet, G.: Emotion regulation profiles in psychogenic non-epileptic seizures. Epilepsy Behav. **23**(3), 364–369 (Mar 2012)
13. Valente, K., Alessi, R., Baroni, G., Marin, R., dos Santos, B., P.A.: The covid-19 outbreak and pnes: The impact of a ubiquitously felt stressor. Epilepsy Behavior **117** (2021)
14. Varone, G., Gasparini, S., Ferlazzo, E., Ascoli, M., Tripodi, G.G., Zucco, C., Calabrese, B., Cannataro, M., Aguglia, U.: A comprehensive machine-learning-based software pipeline to classify eeg signals: A case study on pnes vs. control subjects. Sensors **20**(4) (2020)
15. Vinton, A., Carino, J., Vogrin, S., MacGregor, L., Kilpatrick, C., Matkovic, Z., O'Brien, T.: Convulsive nonepileptic seizures have a characteristic pattern of rhythmic artifact distinguishing them from convulsive epileptic seizures. Epilepsia **45**(11), 1344–1350 (2004)

ICCS Camera Ready Version 2022
To cite this paper please use the final published version:
DOI: 10.1007/978-3-031-08754-7_58